



# The Monocarboxylate transporter inhibitor Quercetin induces intracellular acidification in a mouse model of Glioblastoma Multiforme: in-vivo detection using magnetic resonance imaging

Mohammed Albatany<sup>1,2</sup> · Susan Meakin<sup>3</sup> · Robert Bartha<sup>1,2</sup>

Received: 8 May 2018 / Accepted: 13 July 2018 / Published online: 13 August 2018  
© Springer Science+Business Media, LLC, part of Springer Nature 2018

## Summary

The response of tumor intracellular pH to a pharmacological challenge could help identify aggressive cancer. Chemical exchange saturation transfer (CEST) is an MRI contrast mechanism that is dependent on intracellular pH ( $pH_i$ ).  $pH_i$  is important in the maintenance of normal cell function and is normally maintained within a narrow range by the activity of transporters located at the plasma membrane. In cancer, changes in  $pH_i$  have been correlated with both cell proliferation and cell death. Quercetin is a bioflavonoid and monocarboxylate transporter (MCT) inhibitor. Since MCTs play a significant role in maintaining pH balance in the tumor microenvironment, we hypothesized that systemically administered quercetin could selectively acidify brain tumors. The goals of the current study were to determine whether CEST MRI measurements sensitive to tumor pH could detect acidification after quercetin injection and to measure the magnitude of the pH change ( $\Delta pH$ ). Using a 9.4 T MRI, amine and amide concentration independent detection (AACID) CEST spectra were acquired in six mice approximately  $15 \pm 1$  days after implanting  $10^5$  U87 human glioblastoma multiforme cells in the brain, before and after administration of quercetin (dose: 200 mg/kg) by intraperitoneal injection. Three additional mice were studied as controls and received only vehicle dimethyl sulfoxide (DMSO) injection. Repeated measures *t*-test was used to compare AACID changes in tumor and contralateral tissue regions of interest. Two hours after quercetin injection there was a significant increase in tumor AACID by  $0.07 \pm 0.03$  corresponding to a 0.27 decrease in  $pH_i$ , and no change in AACID in contralateral tissue. There was also a small average increase in AACID in tumors within the three mice injected with DMSO only. The use of the natural compound quercetin in combination with pH weighted MRI represents a unique approach to cancer detection that does not require injection of an imaging contrast agent.

**Keywords** Brain cancer · Glioblastoma multiforme (GBM) · Apoptosis · pH · Quercetin · MRI · CEST

## Abbreviations

GBM	glioblastoma multiforme
$pH_i$	intracellular pH
$pH_e$	extracellular pH
PBS	phosphate buffered saline

CEST	chemical exchange saturation transfer
MCT	monocarboxylate transporter
DMSO	Dimethyl sulfoxide
RF	radiofrequency
$MTR_{asym}$	asymmetric magnetization transfer ratio
MT	magnetization transfer
AACID	amine and amide concentration-independent detection
FSE	fast spin-echo
WASSR	water saturation shift referencing
ROI	region of interest

✉ Robert Bartha  
rbartha@robarts.ca

<sup>1</sup> Centre for Functional and Metabolic Mapping, Robarts Research Institute, The University of Western Ontario, 1151 Richmond Street, London, ON N6A 3K7, Canada

<sup>2</sup> Department of Medical Biophysics, The University of Western Ontario, London, ON N6A 3K7, Canada

<sup>3</sup> Department of Biochemistry, The University of Western Ontario, London, ON N6A 3K7, Canada

## Introduction

The most common primary brain tumors of the central nervous system (CNS) are the gliomas. Glioblastoma multiforme

(GBM) is one of the most aggressive gliomas and lethal brain cancers. The surgical resection of the primary tumor followed by aggressive concurrent radiation and chemotherapy is the current standard of care of GBM tumors [1–4]. However, due to migratory cancer cells that avoid treatment over 90% of GBM tumors recur [4]. Despite advances in therapeutic strategies associated with neurological imaging during treatment, GBM patients often survive only 12–18 months following diagnosis [2–4]. Glioblastomas represent the second leading cause of death among neurological diseases in the United States and one of the greatest challenges in the cure of cancer worldwide [1–4].

A hallmark feature of solid tumors is the maintenance of an alkaline intracellular pH ( $\text{pH}_i$ ) and an acidic extracellular pH ( $\text{pH}_e$ ). The  $\text{pH}_e$  in normal cells is higher (~7.4) than  $\text{pH}_i$  (~7.0–7.1) [5–10]. However, the pH gradient in cancer cells is reversed with lower  $\text{pH}_e$  (~6.7–7.1) than  $\text{pH}_i$  (~7.1–7.3) [5–10]. This altered pH homeostasis is the consequence of increased aerobic glycolysis even in the presence of oxygen; known as the Warburg effect [11]. Although the Warburg effect leads to higher metabolic acid production, cancer cells adaptively increase the expression of regulators that extrude  $\text{H}^+$  and lactate including: carbonic anhydrase, anion exchangers, the  $\text{Cl}^-/\text{HCO}_3^-$  exchangers,  $\text{Na}^+/\text{HCO}_3^-$  co-transporters,  $\text{Na}^+/\text{H}^+$  exchangers, monocarboxylate transporters, the vacuolar (Adenosine Triphosphate)(ATP)ase and ATP synthase [12, 13]. The overexpression of such regulators leads to a relatively alkaline tumor  $\text{pH}_i$ , which supports increased cancer cell proliferation and evasion of apoptosis [14, 15], metastasis of the solid tumor, and can increase tumor resistance to chemotherapy and immunotherapy [16]. Reduction in intracellular pH leads to decreased cell proliferation, induction of apoptosis, and cell death [13, 17].

Targeting the metabolism of solid tumors to change the tumor microenvironment could provide more suitable states for anti-tumor treatment. The modulation of tumor intracellular pH could also be used to predict tumor response to chemotherapy and radiation therapy [3, 12, 18]. Quercetin is a natural compound and an anticancer agent that alters metabolism and  $\text{pH}_i$  [19–21]. Quercetin is a monocarboxylate transporter (MCT) inhibitor [19, 21–24]. It has been characterized as a specific inhibitor of MCT1 and MCT2, and therefore may produce intracellular acidification in tumors by inhibiting lactate and proton transport [19, 21–24]. Quercetin was also found to increase caspase-3 expression inducing apoptosis in glioblastoma cells in vitro [25].

Using chemical exchange saturation transfer (CEST) magnetic resonance imaging (MRI) we have previously shown that several drugs can selectively cause rapid and measurable in-vivo intracellular acidification of glioblastoma. These include lonidamine an MCT inhibitor, topiramate a carbonic anhydrase inhibitor and dichloroacetate, which decreases the expression of MCTs and V-ATPases. To make

these measurements, we applied a CEST technique called amine and amide concentration-independent detection (AACID) that uses the ratio of CEST effects of amide ( $\Delta\omega = 3.5$  ppm) and amine ( $\Delta\omega = 2.75$  ppm) protons to generate  $\text{pH}_i$  dependent contrast, independent of tissue macromolecule concentration and temperature [26]. The CEST contrast originates from exchangeable amine and amide protons that are found in tissue proteins and peptides [27–30]. However the AACID CEST measurement of tissue pH is highly weighted to the intracellular compartment [28] because almost 90% of total protein content exists in the intracellular space [30]. Using AACID-CEST MRI we found a single dose of lonidamine decreased tumor  $\text{pH}_i$  by 0.45 [31], a single dose of topiramate decreased pH by 0.17 [32], and a single dose of dichloroacetate decrease pH by 0.16 [33], approximately one hour after injection. It is important to identify multiple drugs that maximally inhibit key  $\text{pH}_i$ -regulators and glycolytic enzymes to modulate  $\text{pH}_i$  since the effect of a single pharmacologic agent will likely be compensated by other  $\text{pH}_i$  regulatory mechanisms over time.

The purpose of this study was to use AACID-CEST MRI for the acute in-vivo measurement of glioblastoma acidification following quercetin treatment. The measurement of acidification induced by a single dose of drug could help predict tumor response to treatment or potentially provide information on tumor aggressiveness. We hypothesize that a single dose of quercetin will not alter  $\text{pH}_i$  within the contralateral tissue, but will cause intracellular acidification within tumor regions within two hours of treatment due to the inhibition of MCTs.

## Experimental

### Subjects

Nine female Crl:Nu-Foxn1Nu (NU/NU) adult mice (Charles River Laboratories, Canada) were included in the current study and divided into two groups. Six NU/NU mice with U87MG brain tumors were used to evaluate the effect of quercetin on tumor acidification, while three NU/NU mice with U87MG brain tumors were injected with dimethyl sulfoxide (DMSO) as controls. Mice were group housed in ventilated racks, on a 12 h light, 12 h dark cycle. All animal procedures were performed according to a protocol that was consistent with guidelines established by the Canadian Council on Animal Care and was approved by the University of Western Ontario Animal Use Subcommittee.

### Quercetin

Quercetin is a selective MCT inhibitor approved in humans with linear formula  $\text{C}_{15}\text{H}_{10}\text{O}_7$ .

Quercetin was purchased from Sigma–Aldrich (Canada). The drug was dissolved in DMSO. Quercetin was administered by intraperitoneal (i.p.) injection at a dose of 200 mg/kg [34] in a volume of 0.1 ml over the course of 2 min. Control mice with brain tumors received an i.p. injection of DMSO only.

### Animal model of glioblastoma

GBM brain tumors were induced in 22–27 g, NU/NU mice ( $N=6$ ) using U87MG glioma cells established from a human GBM (ATCC; Rockville, MD, USA) as described previously [35]. Briefly, U87MG cells were grown in Dulbecco's modified Eagles' medium supplemented with 10% fetal bovine serum (Wisent Inc., St-Jean-Baptiste, QC, Canada) at 37 °C in a humidified incubator with 5% CO<sub>2</sub> and passaged twice a week. On the day of injection, U87MG cells were washed and dissociated with versene solution (phosphate-buffered saline (PBS) plus 0.5 mM EDTA), then washed twice with PBS, counted and re-suspended to a final concentration of  $1 \times 10^5$  cells in 2 mL PBS. Before injection, mice were anesthetized by inhalation of 4% isoflurane and maintained using 1.5% isoflurane. The mouse was placed in a stereotactic head frame (Stoelting instruments, Wood Dale, IL, USA). The scalp was swabbed with betadine, and an incision was made in the scalp to expose the bregma. A 1 mm diameter hole was drilled at coordinates measured from the bregma (1 mm anterior and 2 mm lateral). U87MG cells (2 ml) were injected at a rate of 0.5  $\mu$ L/min, at a position 3 mm deep from the bregma into the right frontal lobe using a Hamilton (Reno, NV, USA) syringe with a 27-gauge needle attached.

### General mouse preparation for in-vivo imaging

Mice were imaged  $15 \pm 1$  days after cancer cell injection, on a 9.4 T small animal MRI scanner equipped with a 30 mm millipede volume coil (Agilent, Palo Alto, CA, USA). Anesthesia was induced using 4% isoflurane in oxygen and maintained with 1.5%–2.5% isoflurane in oxygen. The mouse was secured on a custom-built MRI-compatible stage, and the head was secured using a bite bar [32] and surgical tape to limit motion due to respiration. The temperature was monitored with a rectal temperature probe, and respiration was monitored with a respiratory sensor pad connected to a pressure transducer that was placed on the thoracic region. Body temperature was maintained at 36.9–37.1 °C throughout imaging by blowing warm air over the animal using a model 1025 small-animal monitoring and gating system (SA Instruments Inc., Stony Brook, NY, USA). Following pre-injection imaging, the mouse was injected with quercetin inside

the MRI by delivering the drug through a fine plastic tube ended with a needle to achieve intraperitoneal injection. All animals were sacrificed immediately after MR imaging.

### In-vivo magnetic resonance imaging

T<sub>2</sub>-weighted images were used for tumor detection acquired using a 2-dimensional fast spin echo pulse sequence (FSE) with parameters: TR/TE = 3000/10 ms, ETL = 4, effective TE = 40 ms, FOV =  $25.6 \times 25.6$  mm<sup>2</sup>, matrix size =  $128 \times 128$ , slice thickness = 1 mm. Two slices from the T<sub>2</sub>-weighted images with maximum tumor coverage (2 mm thickness) were selected upon initial tumor detection for CEST imaging. CEST images were acquired using a fast spin-echo (FSE) pulse sequence (TR/TE = 7000/7 ms, ETL = 32, effective TE = 7 ms, FOV =  $25.6 \times 25.6$  mm<sup>2</sup>, matrix size =  $64 \times 64$ , slice thickness = 2 mm) preceded by a continuous wave radiofrequency (RF) pulse with amplitude 1.5- $\mu$ T and 4 s duration. The CEST images were acquired at different saturation frequencies (from 1.2 to 4.5 ( $\Delta=0.1$ ) ppm, from 5.4 to 6.6 ( $\Delta=0.1$ ) ppm, and -1000 and 1000 ppm images were acquired as a reference, total 49 images). A complete series of CEST images were acquired three times before and three times after drug injection to improve signal-to-noise ratio. For B<sub>0</sub> correction, the water saturation shift referencing (WASSR) technique was used [36]. A linearly spaced 37-point WASSR CEST spectrum with saturation frequencies ranging from -0.6 – 0.6 ppm was acquired using the same pulse sequence except preceded by a short RF saturation pulse (100 ms) with low amplitude (0.2 $\mu$ T). Each WASSR spectrum and CEST spectrum was interpolated to achieve 1-Hz resolution. Each CEST spectrum was then frequency shifted, using the corresponding WASSR spectrum, to account for B<sub>0</sub> variation. B<sub>0</sub> variations were corrected on a pixel-by-pixel basis. The three pre- and three post-injection CEST spectra were summed following B<sub>0</sub> corrections to increase signal to noise ratio.

### CEST data processing

All acquired CEST MR data were analyzed on a pixel-by-pixel basis using custom MATLAB (Mathworks, Natick, MA, USA) code. CEST spectra were smoothed using the 'smooth' algorithm from the MATLAB curve fitting toolbox.

### CEST and contrast calculations

AACID values were measured on a pixel-by-pixel basis using the associated B<sub>0</sub>-corrected and smoothed CEST spectra. The AACID value represents the ratio of the CEST effects of amine protons resonating at 2.75 ppm and amide protons at

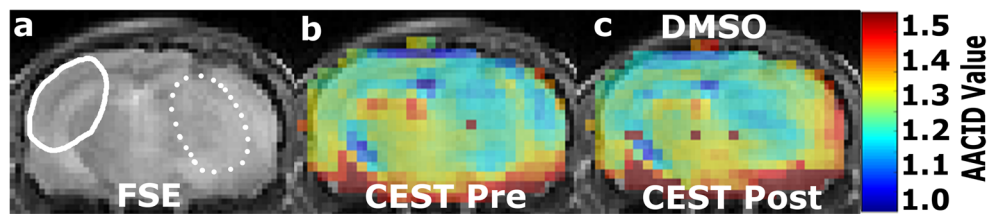


**Fig. 1** Mouse brain with GBM tumor  $15 \pm 1$  days after implantation. (a) Coronal fast spin-echo anatomical image shows regions of interest (ROIs) in the tumor (dotted white line) and on the contralateral side (solid white

line). (b) Baseline AACID map prior to DMSO intraperitoneal injection. (c) The AACID map two hours post DMSO intraperitoneal injection

3.50 ppm, normalized by MT effects measured after saturation at 6.0 ppm and is calculated using Eq. (1) [26].

$$AACID = \frac{M_z(3.50 \text{ ppm}) \times (M_z(6.0 \text{ ppm}) - M_z(2.75 \text{ ppm}))}{M_z(2.75 \text{ ppm}) \times (M_z(6.0 \text{ ppm}) - M_z(3.50 \text{ ppm}))} \quad (1)$$

Following drug administration, the change in pH was estimated by Eq. (2) obtained using the calibration provided by Eq. (8) in McVicar et al. [26].

$$\Delta pH = -4 \times \Delta AACID \quad (2)$$

### Statistical analysis

The regions of interest (ROIs) containing tumor tissue and contralateral tissue were drawn manually based on the signal changes observed in the  $T_2$ -weighted images. The ROIs were manually defined within tumor tissue and contralateral tissue in each mouse brain using MATLAB ('roipoly' function). Average AACID values were calculated at pre injection and post injection of quercetin, within contralateral tissue and tumor regions of interest (ROIs). A paired  $t$ -test was used to calculate differences in mean AACID values measured in the tumor and contralateral ROIs before and after injection of quercetin or DMSO (control).

### Results

AACID CEST maps were acquired in all animals at  $15 \pm 1$  days after U87MG cancer cell implantation. Anatomical FSE MR images were used to identify regions of interest in the tumor and on the contralateral side (Figs. 1a and 2a). AACID CEST maps showed the expected lower AACID value in the tumor region compared to the surrounding tissue (Figs. 1b and 2b) indicating a relatively basic intracellular tumor pH. Fig. 1 shows a typical mouse with brain tumor after injection of DMSO only. There was a small increase in AACID value observed in some brain regions, both within and outside the tumor (Fig. 3a). Examining the average change in the three mice with brain tumors injected with DMSO only, there was a small but significant increase in the average AACID value in the tumor region only (Fig. 4a). Figure 2 shows a typical mouse with brain tumor after injection of quercetin in DMSO. We observed a small increase in AACID value within the tumor (Fig. 2c, Fig. 3b) indicating intracellular acidification within two hours of quercetin injection. On average, there was an increase in the AACID value of  $0.07 \pm 0.03$  ( $N=6$ ,  $p < 0.05$ ) in the tumor region (Fig. 4b) two hours after quercetin injection, but no change in AACID value within the contralateral tissue (Fig. 4b). The measured change in AACID value within the tumor after quercetin injection corresponded to a 0.27 decrease in intracellular pH, estimated using the calibration provided by Eq. 8 in McVicar et al. [26].

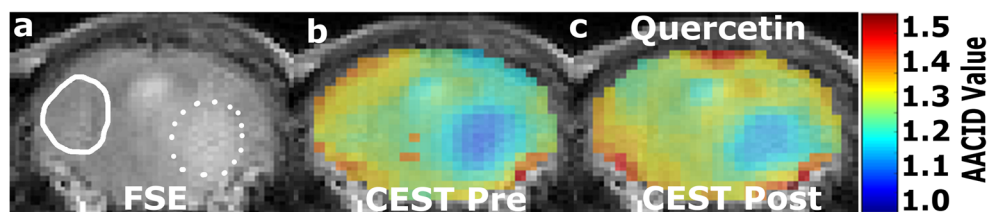
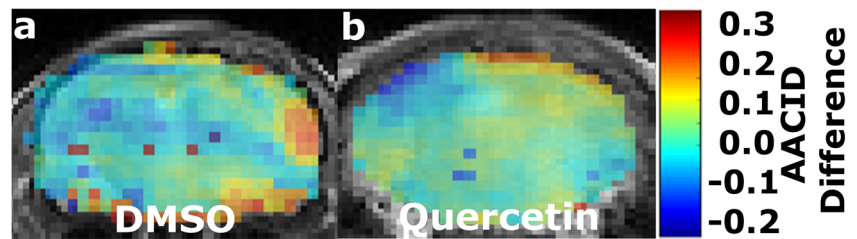


**Fig. 2** Mouse brain with GBM tumor  $15 \pm 1$  days after implantation. (a) Coronal fast spin-echo anatomical image shows regions of interest (ROIs) in the tumor (dotted white line) and on the contralateral side (solid white

line). (b) Baseline AACID map prior to quercetin injection. (c) The AACID map two hours post quercetin (200 mg/kg) intraperitoneal injection

**Fig. 3** Mouse brain AACID difference maps for examples shown in Figs. 1 and 2. (a) Post -pre DMSO injection and, (b) Post -pre quercetin (200 mg/kg) intraperitoneal injection



## Discussion

This study is the first to demonstrate intracellular acidification in brain tumors within the first two hours after injection of a single dose of quercetin (200 mg/kg) in DMSO. In contrast, there was no change in AACID detected on the side contralateral to the tumor after quercetin injection. The purpose of this study was to determine whether CEST MRI measurement of tumor AACID value could detect acidification after quercetin injection and to measure the magnitude of the AACID value changes in orthotopic GBM tumor. The results indicate that the AACID CEST method is sensitive to quercetin-induced pH changes in tumors within two hours of treatment. This use of a pharmacologic agent to induce a measurable physiologic change represents a unique approach to cancer detection that differs from other current molecular imaging techniques. Decreasing intracellular pH could also increase the response of the tumor to hyperthermia, radiation, and chemotherapy treatments [37, 38].

Quercetin is a natural compound and an anticancer agent that alters metabolism and  $\text{pH}_i$ . Quercetin is an inhibitor of monocarboxylate transporters (MCTs) [19, 21–24]. The results of the current study are consistent with previous work that has shown decreased  $\text{pH}_i$  following quercetin treatment [19]. Quercetin could both precede and be given concurrently with chemotherapy or radiation therapy, to potentially increase their effectiveness, decrease the required doses, and limit the toxicity of these standard therapies [39].

In previous studies using the same methodology to evaluate the magnitude of tumor acidification, we found lonidamine

decreased intracellular pH by 0.25 at a dose of 50 mg/kg and decreased intracellular pH by 0.45 at a dose of 100 mg/kg [31]. Topiramate decreased intracellular pH by 0.17 [32]. More recently we also showed that giving 200 mg/kg of dichloroacetate, which decreases the expression of monocarboxylate transporters and V-ATPases, decreased intracellular pH by 0.16 [33]. The quercetin dose (200 mg/kg) used in the current study is commonly used in the literature for animal studies [34]. At the dose studied, quercetin caused intracellular pH to decrease by 0.27. Although quercetin was less effective than lonidamine, lonidamine is toxic and can't be used in humans.

The current study has several limitations that should be considered. First, the number of animals used was small. However, the effect sizes were large, and the ROI based pH measurements had low intra-subject variability. Not surprisingly, the standard error of the mean of the pH measurements appeared larger in the control animals, since only three animals were used in the control group, compared to six animals in the treated group. The biological effect of DMSO may also have caused some variability in the tumor pH depending on the uptake of the compound. It is important to note that the statistical comparisons made between groups utilized a test-retest design to reduce the impact of this inter-subject variation. Therefore, the animal numbers used were sufficient to determine whether quercetin produced a measurable pH effect. Second, quercetin (200 mg/kg) could not be dissolved in distilled water or PBS. Therefore we dissolved quercetin in DMSO. DMSO alone caused a small increase in AACID value suggesting it induces intracellular acidification. Although

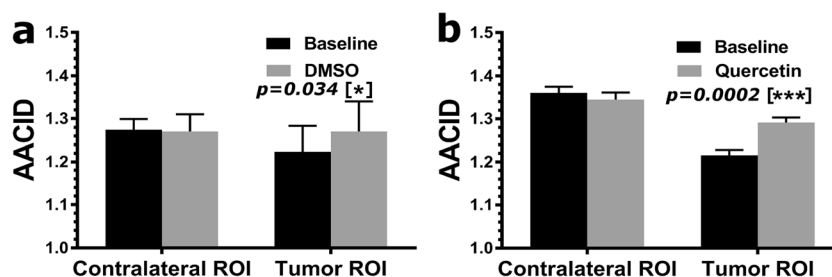


**Fig. 4** Average AACID value in tumor and contralateral ROIs: **a** Pre and post intraperitoneal DMSO injection used as a control condition ( $N=3$ ). There was no change in AACID value within the contralateral ROI, however a small significant increase in the average AACID value was observed within the tumor ROI. **b** Pre and post quercetin 200 mg/kg

intraperitoneal injection ( $N=6$ ). A larger significant increase in AACID value was observed within the tumor ROI after DMSO+quercetin injection indicating intracellular acidification. Error bars represent the standard error of the mean. The asterisks indicated  $p < 0.05$  in repeated measures t-test

the mechanism for this effect cannot be defined from the current study, DMSO can interact with the cell plasma membrane enhancing pore formation and increasing cell permeability [40]. This change in cell permeability could impact on ion transport, which in turn may modify tumor pH. The efficacy of DMSO in tumors is likely due to the high expression of ion transporters in cancer. Third, we did not optimize the quercetin dose in the current study, only the a single of 200 mg/kg of quercetin was examined. Future studies should determine whether higher doses of quercetin could increase tumor acidification and whether the effect is repeatable after multiple exposures.

The use of CEST MRI contrast to detect changes in intracellular pH has many potential applications in cancer detection and treatment evaluation [3, 28, 41]. The results of the current study demonstrate that acute CEST MRI contrast changes after administration of quercetin could help localize brain cancer by rapidly and selectively inducing a shift in intracellular pH.

**Acknowledgements** Funding for this study was provided by the Ontario Institute of Cancer Research (OICR) Smarter Imaging Program and the Canadian Institutes of Health Research (CIHR). MRI facilities were supported by Brain Canada and the Canada First Research Excellence Fund (BrainsCAN). Thanks to Misan University-Ministry of Higher Education and Scientific Research, Iraq.

**Funding** This study was funded by the Ontario Institute of Cancer Research (OICR) Smarter Imaging Program (grant number 00807).

## Compliance with ethical standards

**Conflict of interest** The authors declare no conflict of interest.

**Ethical approval** All applicable national and institutional guidelines for the care and use of animals were followed. All procedures performed in studies involving animals were in accordance with the ethical standards of the institution or practice at which the studies were conducted.

## References

- Kanu OO, Mehta A, Di C, Lin N, Bortoff K, Bigner DD, Yan H, Adamson DC (2009) Glioblastoma multiforme: a review of therapeutic targets. *Expert Opin Ther Targets* 13(6):701–718. <https://doi.org/10.1517/14728220902942348>
- Wen PY, Kesari S (2008) Malignant gliomas in adults. *N Engl J Med* 359(5):492–507. <https://doi.org/10.1056/NEJMra0708126>
- Sagiya K, Mashimo T, Togao O, Vemireddy V, Hatanpaa KJ, Maher EA, Mickey BE, Pan E, Sherry AD, Bachoo RM, Takahashi M (2014) In vivo chemical exchange saturation transfer imaging allows early detection of a therapeutic response in glioblastoma. *Proc Natl Acad Sci U S A* 111(12):4542–4547. <https://doi.org/10.1073/pnas.1323855111>
- Easaw JC, Mason WP, Perry J, Laperriere N, Eisenstat DD, Del Maestro R, Belanger K, Fulton D, Macdonald D, Canadian Glioblastoma Recommendations C (2011) Canadian recommendations for the treatment of recurrent or progressive glioblastoma multiforme. *Curr Oncol* 18(3):e126–e136
- Gerweck LE, Seetharaman K (1996) Cellular pH gradient in tumor versus normal tissue: potential exploitation for the treatment of cancer. *Cancer Res* 56(6):1194–1198
- Stubbs M, Bhujwalla ZM, Tozer GM, Rodrigues LM, Maxwell RJ, Morgan R, Howe FA, Griffiths JR (1992) An assessment of 31P MRS as a method of measuring pH in rat tumours. *NMR Biomed* 5(6):351–359
- Ha DH, Choi S, Oh JY, Yoon SK, Kang MJ, Kim KU (2013) Application of 31P MR spectroscopy to the brain tumors. *Korean J Radiol* 14(3):477–486. <https://doi.org/10.3348/kjr.2013.14.3.477>
- Cichocka M, Kozub J, Urbanik A (2015) PH Measurements of the Brain Using Phosphorus Magnetic Resonance Spectroscopy (31PMRS) in Healthy Men – Comparison of Two Analysis Methods. *Pol J Radiol*. <https://doi.org/10.12659/PJR.895178>
- Oberhaensli RD, Galloway GJ, Hilton-Jones D, Bore PJ, Styles P, Rajagopalan B, Taylor DJ, Radda GK (1987) The study of human organs by phosphorus-31 topical magnetic resonance spectroscopy. *Br J Radiol* 60(712):367–373. <https://doi.org/10.1259/0007-1285-60-712-367>
- Maintz D, Heindel W, Kugel H, Jaeger R, Lackner KJ (2002) Phosphorus-31 MR spectroscopy of normal adult human brain and brain tumours. *NMR Biomed* 15(1):18–27
- Gatenby RA, Gillies RJ (2004) Why do cancers have high aerobic glycolysis? *Nat Rev Cancer* 4(11):891–899. <https://doi.org/10.1038/nrc1478>
- Huber V, De Milito A, Harguindey S, Reshkin SJ, Wahl ML, Rauch C, Chiesi A, Pouyssegur J, Gatenby RA, Rivoltini L, Fais S (2010) Proton dynamics in cancer. *J Transl Med* 8:57. <https://doi.org/10.1186/1479-5876-8-57>
- Neri D, Supuran CT (2011) Interfering with pH regulation in tumours as a therapeutic strategy. *Nat Rev Drug Discov* 10(10):767–777. <https://doi.org/10.1038/nrd3554>
- Webb BA, Chimenti M, Jacobson MP, Barber DL (2011) Dysregulated pH: a perfect storm for cancer progression. *Nat Rev Cancer* 11(9):671–677. <https://doi.org/10.1038/nrc3110>
- Shrode LD, Tapper H, Grinstein S (1997) Role of intracellular pH in proliferation, transformation, and apoptosis. *J Bioenerg Biomembr* 29(4):393–399
- Barar J, Omid Y (2013) Dysregulated pH in tumor microenvironment checkmates Cancer therapy. *Bioimpacts* 3(4):149–162. <https://doi.org/10.5681/bi.2013.036>
- Izumi H, Torigoe T, Ishiguchi H, Uramoto H, Yoshida Y, Tanabe M, Ise T, Murakami T, Yoshida T, Nomoto M, Kohno K (2003) Cellular pH regulators: potentially promising molecular targets for cancer chemotherapy. *Cancer Treat Rev* 29(6):541–549. [https://doi.org/10.1016/s0305-7372\(03\)00106-3](https://doi.org/10.1016/s0305-7372(03)00106-3)
- Wood PJ, Sansom JM, Newell K, Tannock IF, Stratford IJ (1995) Reduction of tumour intracellular pH and enhancement of melphalan cytotoxicity by the ionophore Nigericin. *Int J Cancer* 60(2):264–268
- Volk C, Kempfski B, Kempfski OS (1997) Inhibition of lactate export by quercetin acidifies rat glial cells in vitro. *Neurosci Lett* 223(2):121–124
- Srivastava S, Somasagara RR, Hegde M, Nishana M, Tadi SK, Srivastava M, Choudhary B, Raghavan SC (2016) Quercetin, a natural flavonoid interacts with DNA, arrests cell cycle and causes tumor regression by activating mitochondrial pathway of apoptosis. *Sci Rep* 6:24049. <https://doi.org/10.1038/srep24049>
- Izumi H, Takahashi M, Uramoto H, Nakayama Y, Oyama T, Wang KY, Sasaguri Y, Nishizawa S, Kohno K (2011) Monocarboxylate transporters 1 and 4 are involved in the invasion activity of human lung cancer cells. *Cancer Sci* 102(5):1007–1013. <https://doi.org/10.1111/j.1349-7006.2011.01908.x>
- Perez-Escuredo J, Van Hee VF, Sboarina M, Falces J, Payen VL, Pellerin L, Sonveaux P (2016) Monocarboxylate transporters in the

- brain and in cancer. *Biochim Biophys Acta* 1863(10):2481–2497. <https://doi.org/10.1016/j.bbamcr.2016.03.013>
23. Kim JH, Kim SH, Alfieri AA, Young CW (1984) Quercetin, an inhibitor of lactate transport and a hyperthermic sensitizer of HeLa cells. *Cancer Res* 44(1):102–106
  24. McKay TB, Lyon D, Sarker-Nag A, Priyadarsini S, Asara JM, Karamichos D (2015) Quercetin attenuates lactate production and extracellular matrix secretion in keratoconus. *Sci Rep* 5:9003. <https://doi.org/10.1038/srep09003>
  25. Sang DP, Li RJ, Lan Q (2014) Quercetin sensitizes human glioblastoma cells to temozolomide in vitro via inhibition of Hsp27. *Acta Pharmacol Sin* 35(6):832–838. <https://doi.org/10.1038/aps.2014.22>
  26. McVicar N, Li AX, Goncalves DF, Bellyou M, Meakin SO, Prado MA, Bartha R (2014) Quantitative tissue pH measurement during cerebral ischemia using amine and amide concentration-independent detection (AACID) with MRI. *J Cereb Blood Flow Metab* 34(4):690–698. <https://doi.org/10.1038/jcbfm.2014.12>
  27. Zong X, Wang P, Kim SG, Jin T (2014) Sensitivity and source of amine-proton exchange and amide-proton transfer magnetic resonance imaging in cerebral ischemia. *Magn Reson Med* 71(1):118–132. <https://doi.org/10.1002/mrm.24639>
  28. Zhou JY, Payen JF, Wilson DA, Traystman RJ, van Zijl PCM (2003) Using the amide proton signals of intracellular proteins and peptides to detect pH effects in MRI. *Nat Med* 9(8):1085–1090. <https://doi.org/10.1038/nm907>
  29. Zhou JLB, Wilson DA, Lartera J, van Zijl PC (2003) Amide proton transfer (APT) contrast for imaging of brain tumors. *Magn Reson Med* 50:1120–1126. <https://doi.org/10.1002/mrm.10651>
  30. Murray RK GD (2003) *Membranes: structure & function*. McGraw-Hill Companies, Inc:415–433
  31. McVicar N, Li AX, Meakin SO, Bartha R (2015) Imaging chemical exchange saturation transfer (CEST) effects following tumor-selective acidification using Ionidamine. *NMR Biomed* 28(5):566–575. <https://doi.org/10.1002/nbm.3287>
  32. Marathe K, McVicar N, Li A, Bellyou M, Meakin S, Bartha R (2016) Topiramate induces acute intracellular acidification in glioblastoma. *J Neuro-Oncol* 130(3):465–472. <https://doi.org/10.1007/s11060-016-2258-y>
  33. Albatany M, Li A, Meakin S, Bartha R (2017) Dichloroacetate induced intracellular acidification in glioblastoma: in vivo detection using AACID-CEST MRI at 9.4 tesla. *Journal of Neuro-oncology*. <https://doi.org/10.1007/s11060-017-2664-9>
  34. Reddy NS, Nirmala P, Chidambaram N, Kumar P, Nagar A (2012) Quercetin in dimethyl benzanthracene induced breast cancer in rats. *Am J Pharmacol Toxicol* 7(2):68–72
  35. Li AX, Suchy M, Li C, Gati JS, Meakin S, Hudson RH, Menon RS, Bartha R (2011) In vivo detection of MRI-PARACEST agents in mouse brain tumors at 9.4 T. *Magn Reson Med* 66(1):67–72. <https://doi.org/10.1002/mrm.22772>
  36. Kim M, Gillen J, Landman BA, Zhou J, van Zijl PC (2009) Water saturation shift referencing (WASSR) for chemical exchange saturation transfer (CEST) experiments. *Magn Reson Med* 61(6):1441–1450. <https://doi.org/10.1002/mrm.21873>
  37. Park HJ, Makepeace CM, Lyons JC, Song CW (1996) Effect of intracellular acidity and ionomycin on apoptosis in HL-60 cells. *Eur J Cancer* 32A(3):540–546
  38. Park HJ, Lyons JC, Ohtsubo T, Song CW (1999) Acidic environment causes apoptosis by increasing caspase activity. *Br J Cancer* 80(12):1892–1897. <https://doi.org/10.1038/sj.bjc.6690617>
  39. Jakubowicz-Gil J, Langner E, Wertel I, Piersiak T, Rzeski W (2010) Temozolomide, quercetin and cell death in the MOGGCCM astrocytoma cell line. *Chem Biol Interact* 188(1):190–203. <https://doi.org/10.1016/j.cbi.2010.07.015>
  40. Notman R, Noro M, O'Malley B, Anwar J (2006) Molecular basis for dimethylsulfoxide (DMSO) action on lipid membranes. *J Am Chem Soc* 128(43):13982–13983. <https://doi.org/10.1021/ja063363t>
  41. Zhou J, Tryggstad E, Wen Z, Lal B, Zhou T, Grossman R, Wang S, Yan K, Fu DX, Ford E, Tyler B, Blakeley J, Lartera J, van Zijl PC (2011) Differentiation between glioma and radiation necrosis using molecular magnetic resonance imaging of endogenous proteins and peptides. *Nat Med* 17(1):130–134. <https://doi.org/10.1038/nm.2268>